

# **Biomimetic growth of apatite on titania nanotube arrays fabricated by titanium anodization in $\text{NH}_4\text{F}/\text{H}_2\text{SO}_4$ electrolyte**

TIAN TIAN, XIAO XIU-FENG, SHE HOU-DE, LIU RONG-FANG\*

College of Chemistry and Material Science, Fujian Normal University, Fuzhou 350007, China

Titania nanotube arrays were fabricated by anodizing titanium in  $\text{NH}_4\text{F}/\text{H}_2\text{SO}_4$  electrolyte. The crystal structure and apatite-forming ability of the titania nanotube arrays were investigated. The samples were examined by ESEM, XRD and FT-IR. The results indicate that the crystal structure of the titania nanotube arrays transformed from amorphous to anatase and rutile ones upon rising the temperature of annealing. The surface structure of the nanotube arrays could enhance the bioactivity of titania. The bioactivity of titania nanotube arrays depends on their crystal structure, diminishing in the following series: mixture of anatase and rutile structure > anatase > amorphous.

Key words: *titania; nanotube array; apatite; bioactivity*

## **1. Introduction**

Titanium and its alloys are used as a common material for bone implants under biomechanical loading conditions due to their excellent mechanical properties and biocompatibility [1, 2] despite their poor bonding ability. In order to improve the bone bonding ability of titanium implants, many attempts have been made to modify the chemistry composition and structure of titanium surfaces. These methods include dip coating [3], plasma spraying [4,5], magnetron sputtering [6], ion implanting [7], electrocrystallization [8], electrophoretic deposition [9], hydrothermal electrodeposition [10], anode oxidation [11], acid etching [12], oxidation with hydrogen peroxide [13], sol-gel methods [14,15], alkali-heating procedure [16], acid-alkali or precalcification procedure [17,18], and surface-induced mineralization [19]. Plasma spraying is one of the most widely investigated methods for titanium coating but the major problem is that it is a line of sight process, and the coating is nonuniform and heterogeneous.

---

\*Corresponding author, e-mail: [rfliu@vip.sina.com](mailto:rfliu@vip.sina.com)

Another problem is that the HA powder is heated at extremely high temperature and deposited with very high velocity on the metal surface. Furthermore, the composition and crystallinity of HA are difficult to control. Naturally, it is believed that an ideal bioactive method, simple and cost-effective, should be employed.

Recently, it has been reported that bioactive titanium surface can be prepared by fabricating a titania nanotube array layer on the surface of titanium [29]. Tsuchiya et al. [29] reported that the presence of the titania nanotube arrays on a titanium surface enhanced the apatite formation. In this paper, a layer of titania nanotube arrays was obtained *via* anodic oxidation on titanium in  $\text{NH}_4\text{F}/\text{H}_2\text{SO}_4$  electrolyte. The bioactivities of the layers annealed at various temperatures with various crystal structures were studied by soaking 1.5 times simulated body fluid (1.5 SBF).

## 2. Experimental

Titanium foils (99.5% pure) were purchased from the Northwest Institute For Non-Ferrous Metal Research (China). Prior to anodization, the titanium foils were ultrasonically cleaned in acetone and distilled water for 5 min, respectively, and then eroded in 4 wt. %  $\text{HF}$ –5 M  $\text{HNO}_3$  for 30 s followed by ultrasonic cleaning in distilled water for 5 min and dried in air at 40 °C. A two-electrode arrangement with a graphite cathode was used. 1.75 M  $\text{H}_2\text{SO}_4$  solutions with 0.5 wt. %  $\text{NH}_4\text{F}$  were used as an electrolyte. The anodizing voltage was kept constant at 20 V during the entire process with a DC power supply (GOA, China). The whole course of anodization was conducted at room temperature (25 °C) with magnetic agitation. The samples were dried at 40 °C in air, and then annealed at various temperatures (from 300 °C to 600 °C) for 4 h in a furnace with air.

The bioactivity study was carried out by inserting the as-prepared sample into culture vials containing simulated body fluid (1.5 SBF) for 9 days at 37 °C without stirring. The composition of the 1.5 SBF was reported as Kukubo [20] but the quantity of Ca and P added was 1.5 times greater to shorten the period of the bioactivity study. The samples were taken out, washed with distilled water and dried in air at 40 °C before coating characterization.

Philips XL30 ESEM was employed for the structural and morphological characterization of the sample. X-ray diffraction measurements were performed on Philips X'Pert MPD diffractometer with  $\text{CuK}_\alpha$  radiation, the X-ray generator operated at 40 kV and 40 mA. Data sets were collected over the range of 5–90° with a step size of 0.02° and a count rate of 4.0 °/min. Identification of phases was achieved by comparing the diffraction patterns of the samples with ICDD (JCPDS) standards. FT-IR spectra were obtained by using an Nicolet Avatar 360 spectrometer at the resolution of 4  $\text{cm}^{-1}$ .

## 3. Results and discussion

Figure 1 shows the surface morphology and cross-sections of the titania nanotube arrays fabricated by anodizing titanium in 1.75 M  $\text{H}_2\text{SO}_4$  solutions with 0.5 wt. %

$\text{NH}_4\text{F}$ . It is clear that the surface of the titania nanotube layer is flat and smooth with discrete, hollow, cylindrical, tubular features. The nanotubes of the arrays possess the inner diameter of about 120 nm and the length of ca. 300 nm. This structure possesses larger surface areas and is different from the nonporous  $\text{TiO}_2$  layers formed from other electrolytes, such as sulfuric acid [21, 22]. In fluoride-containing electrolytes, the anodization of titanium is accompanied with its chemical dissolution due to the formation of  $\text{TiF}_6^{2-}$ . Highly uniform nanotube arrays, instead of nonporous structure, were formed [23, 24].

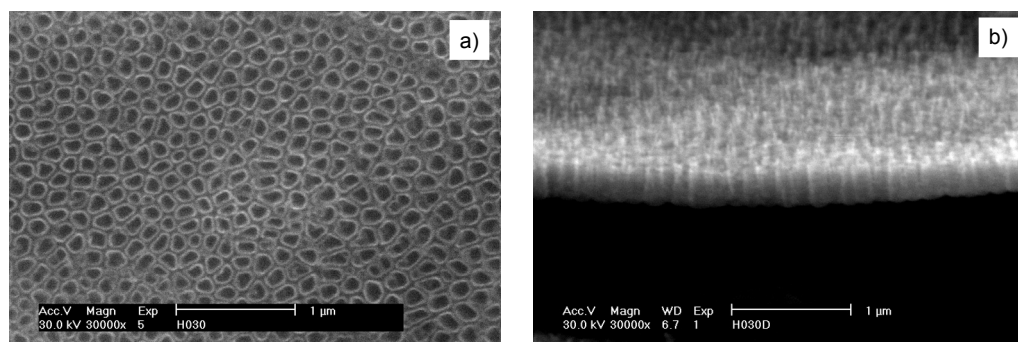


Fig. 1. The surface morphology (a) and cross-section (b) of the titania nanotube arrays

To evaluate the potential use of the titania nanotube layers as coatings for biomedical implants, the as-prepared titania nanotube layers were annealed at various temperatures and then soaked in 1.5 SBF. The microstructures of the nanotube arrays annealed from 300 °C to 600 °C were observed by ESEM. There were no discernible changes in the tube diameters or wall thicknesses after annealing at 300 °C for 4 h. A little diminishing of the tube diameter occurred at 500 °C. As temperature raised to 600 °C, obvious breakage occurred as shown in Fig. 2.

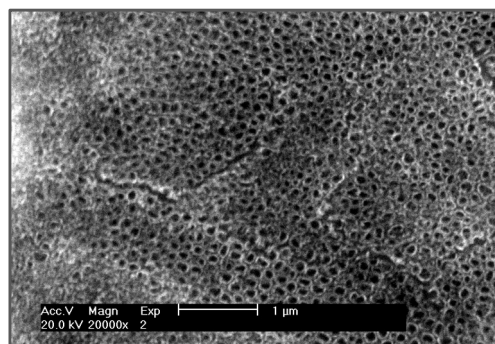


Fig. 2. The surface morphology of the nanotube arrays after annealing at 600 °C

Figure 3 shows the XRD patterns of the sample annealed at different temperatures. The as-prepared titania nanotube arrays were found to be amorphous (curve e). It is clear that the sample crystallized in the anatase phase at the temperature close to

300 °C (curve b). The diffraction peak of anatase phase is enhanced at 500 °C (curve c). When the temperature approaches 600 °C (curve d), the rutile phase emerges in the X-ray diffraction pattern. The same heat treatment was performed on pure titanium without titania nanotube arrays. There is only Ti peak appearing on the pattern at 500°C. The rutile phase emerges in the X-ray diffraction pattern straightly at 600°C (curve a).

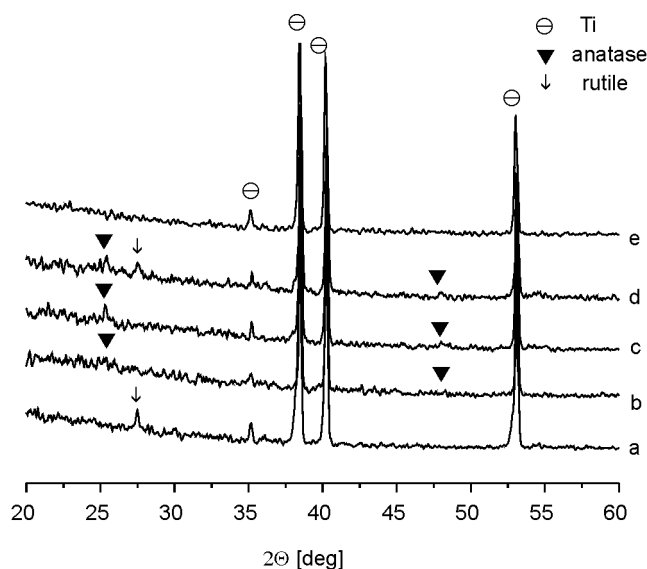


Fig. 3. XRD patterns of unanodized titanium (a) and the titania nanotubes arrays annealed at: b) 300 °C c) 500 °C, d) 600 °C, e) unannealed

The results indicate that the crystallization of titania nanotube arrays changes as the annealing temperature rises. The changes in morphologies of the titania nanotube arrays at high temperatures are the result of crystallization of titania nanotube arrays and oxidation of titanium substrate. Anatase and rutile are two ordinary phases of titania; both belong to tetragonal structures but there are four  $\text{TiO}_2$  molecules in the unit cell of anatase, two in that of rutile. Oxygen octahedra are joined together *via* face in anatase, *via* culmination in rutile. According to the third principle of Pauling [20], the presence of shared polyhedral edges and especially shared polyhedral faces decreases the stability of the crystal structure. Thus the crystal phase of titania nanotube arrays could transform from anatase to rutile as the temperature is increased.

The surface morphologies of the annealed titania nanotube arrays after soaking in 1.5 SBF are shown in Fig. 4. There are no obvious changes on the surface of the unannealed titania nanotube arrays (Fig. 4a), and the mouths of the nanotubes are clearly visible. For the samples annealed at 300 °C (Fig. 4b), only a small amount of particles formed sparsely scattered on the surface of the sample and could only be detected with ESEM. The morphology is very similar to that of the deposited apatite on a substrate

through biomimetic processing utilizing SBF [26]. These particles were thus regarded as apatite. For the samples annealed at 500 °C (Fig. 4c) and 600 °C (Fig. 4d), a new layer formed on the surface of the titania nanotube arrays. The new layer formed at 600 °C is more compact than that formed at 500 °C.

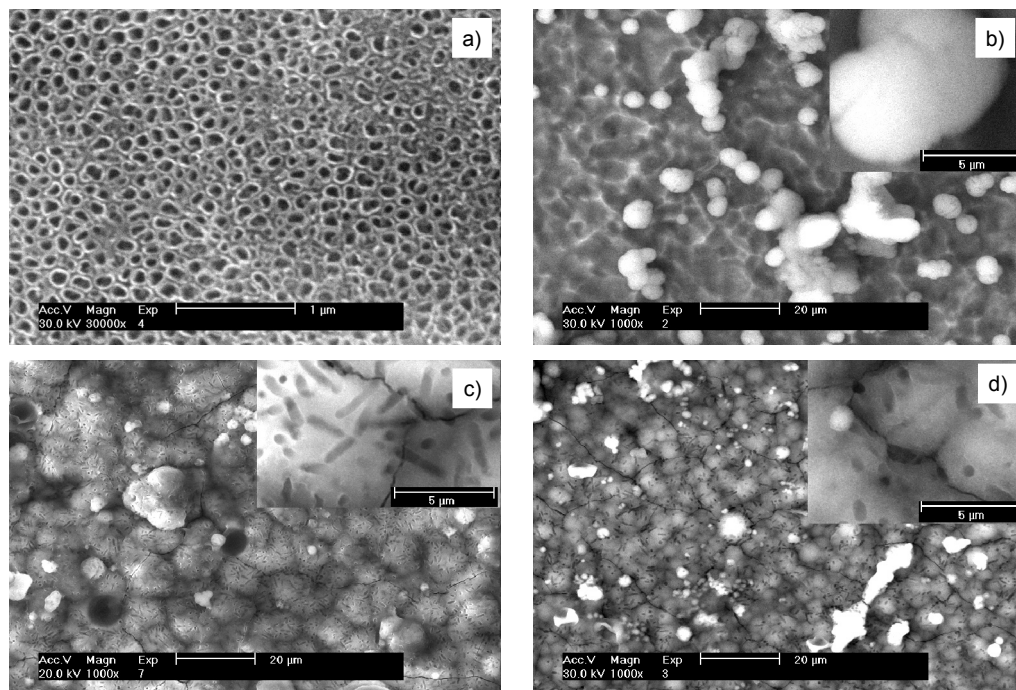


Fig. 4. SEM images of the samples soaked in 1.5 SBF unannealed (a) and annealed at 300 °C (b), 500 °C (c) and 600 °C (d)

The XRD pattern of the layer is shown in Fig. 5 and compared with the standard card (JCPDS 09-432), indicating that the layer formed on the surface of titania nanotubes is an apatite layer. The FT-IR spectra of the new layer formed on the nanotube surface annealed at 500 °C and 600 °C are shown in Fig. 6. The new formed layer exhibited sharp P–O asymmetric stretching mode of  $\text{PO}_4^{3-}$  group at  $1027\text{ cm}^{-1}$ , triple and double degenerated bending modes of phosphate O–P–O bands at 607, 568, and  $470\text{ cm}^{-1}$  and modes of  $\text{CO}_3^{2-}$  group at 1458, 1418, and  $871\text{ cm}^{-1}$ . A broad absorption band at  $3451\text{ cm}^{-1}$  and the bending mode at  $1652\text{ cm}^{-1}$  are the bands of  $\text{H}_2\text{O}$ . The results indicate that the apatite formed on the nanotube arrays layer is B-type carbonated apatite, in which  $\text{PO}_4^{3-}$  groups are partly substituted by  $\text{CO}_3^{2-}$ .

Based on the above analyses, the bioactivity of titania nanotube arrays layer was ranked in the following series: annealed at 600 °C > annealed at 500 °C > annealed at 300 °C > unannealed. The apatite deposition on titania has been reported by Healy and

Ducheyne [27]. They have suggested that titanium was subjected to passive dissolution in SBF and within a soaking period up to 400h, the passive dissolution was governed by the hydrolysis of titania, which resulted in the formation of  $\text{OH}^-$  and  $\text{Ti}(\text{OH})_n^{(4-n)+}$ . The  $\text{OH}^-$  ions were adsorbed on the oxide surface forming Ti–OH groups, and subsequently promote the nucleation of apatite on the surface of titanium.

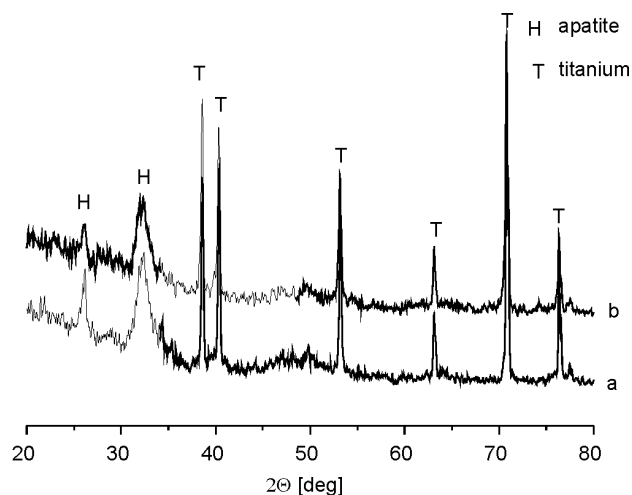


Fig. 5. XRD patterns of the samples soaked in 1.5 SBF annealed at 500 °C (a), and 600 °C (b)

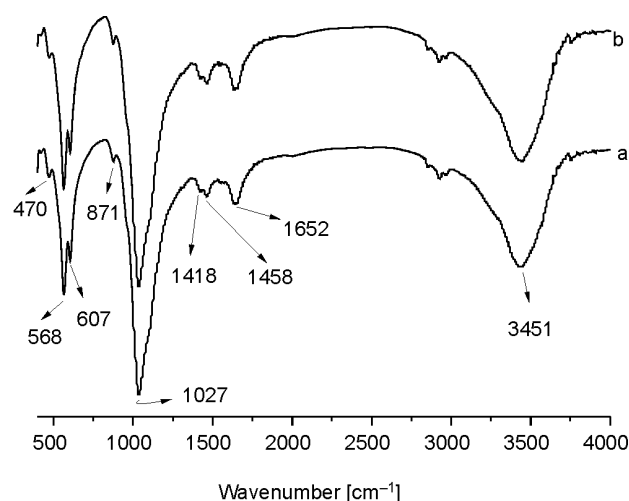


Fig. 6. FT-IR spectra of the new formed layer after soaking in SBF for 9 days:  
a) the nanotube arrays with anatase phase annealed at 500 °C,  
b) the nanotube arrays with a mixture of anatase and rutile phase annealed at 600 °C

The forming of the Ti–OH groups is the key factor for the nucleation of apatite. However, the bioactivity of the titania nanotube arrays is distinguished due to different

crystal structure at present. The results imply that not all Ti-OH groups, but certain type of Ti-OH groups in a specific structural arrangement, are effective in inducing apatite nucleation. The amorphous structure cannot induce apatite formation on their surface in SBF, whereas the anatase structure is able to induce apatite formation. However, the mixture of anatase and rutile structure possesses a better capability for the formation of apatite than the former structure. This phenomenon has been reported by Uchida [28] who found that the titania gels with an amorphous structure did not induce apatite formation on their surfaces in SBF, whereas gels with an anatase or rutile structure induced apatite formation on their surfaces. Thus the bioactivity of the titania nanotube arrays lies on the crystal structure, mixture of anatase and rutile structure > anatase > amorphous.

The control experiment has been carried out by Tsuchiya et al. [29]. They reported that on the compact anodic titania layer, which was obtained in  $\text{H}_2\text{SO}_4$  solutions and annealed at 550 °C, there is no apatite layer formed after soaking in the 1.5SBF. The result implied that the porous structure of the titania nanotube arrays layer is advantageous to the nucleation of apatite because the porous nature of the titania nanotube arrays layer enhances the anchorage of the nucleation of apatite and opened up the possibility of the incorporation on the titanium.

#### 4. Conclusions

The titania nanotube arrays were fabricated by titanium anodization in  $\text{NH}_4\text{F}/\text{H}_2\text{SO}_4$  electrolyte. The crystal structure of the arrays was transformed from amorphous to anatase and rutile after annealing at various temperatures. The bioactivity study was carried out by soaking the samples in 1.5 SBF. The results show that the titania nanotube arrays with a mixture of anatase and rutile structure possess a high apatite forming ability, implying that titania nanotube arrays with a specific crystal structures such as anatase, mixture of anatase and rutile, are effective for apatite formation. These results suggest the bioactive titanium to be used as an implant material may be obtained by anodic oxidation and subsequent annealing.

#### Acknowledgements

The authors express their gratitude to the National Nature Science Foundation of China (30600149), the Science Research Foundation of Ministry of Health and United Fujian Provincial Health and Education Project for Tackling the Key Research, P.R. China (WKJ 2005-2-008) and Fujian Development and Reform Commission of China (No. 2004 [477]).

#### References

- [1] LONG M., RACK H.J., *Biomater.*, 19 (1998), 1621.
- [2] BRUNETTE D.M., TENGVALL P., TEXTOR M., THOMSEN P., *Titanium in Medicine*, Springer Verlag Berlin, 2001, p.13

- [3] LEE J., AOKI H., Biomed. Mater. Eng., 5 (1995), 49.
- [4] GROOT K.D., GEESINK R., KLEIN C., SEREKIAN P., J. Biomed. Mater. Res., 21 (1987), 1375.
- [5] CHEN J., TONG W., CAO Y., FENG J., ZHANG X., J. Biomed. Mater. Res., 34 (1997), 15.
- [6] OZEKI K., YUHTA T., AOKI H., NISHIMURA I., FUKUI Y., Biomed. Mater. Eng., 10 (2000), 221.
- [7] PHAM M.T., MAITZ M.F., MATZ W., REUTHER H., RICHTER E., STEINER G., Thin Solid Films, 379 (2000), 50.
- [8] SHIRKHANZADEH M., J. Mater. Sci. Mater. Med., 6 (1995), 90.
- [9] ZITOMIRSKY I., GOL-OR L., ISRAL I., J. Mater. Sci. Mater. Med., 8 (1997), 213.
- [10] XIAO X.F., LIU R.F., ZHENG Y.Z., Mater. Lett., 59 (2005), 1660.
- [11] ISHIZAWA H., OGINO M., J. Biomed. Mater. Res., 34 (1997), 15.
- [12] MORRA M., CASSINELLI C., BRUZZONE G., CARPI A., DI SANTI G., GIARDINO R., FINI M., Int. J. Oral. Maxillofac Implants, 18 (2003), 40.
- [13] TENGVALL P., ELWING H., LUNDSTROM I., J. Colloid Inter. Sci., 130 (1989), 405.
- [14] LI P., OHTSUKI C., KOKUBO T., NANKANISHI K., SOGA N., GROOT K.D., J. Biomed. Mater. Res., 28 (1994), 7.
- [15] PELTOLA T., PATSI M., RAHIALA H., KANGASNIEMI I., YLI-URPO A., J. Biomed. Mater. Res., 41 (1998), 504.
- [16] KIM H.M., MIYAJI F., KOKUBO T., NAKAMURA T., J. Biomed. Mater. Res., 38 (1997), 121.
- [17] WEN H.B., WOLKE J.G.C., WIJN J.R.D., LIU Q., CUI F.Z., GROOT K.D., Biomater., 18 (1997), 1471.
- [18] WEN H.B., LIU Q., WIJN J.R.D., GROOT K.D., J. Mater. Sci. Mater. Med., 8 (1998), 121.
- [19] BUNKER B.C., RIEKE P.C., TARASEVICH B.J., CAMPBELL A.A., FRYXELL G.E., GRAFF G.L., SONG L., LIU S., VIRDEN J.W., MCVAY G.L., Science, 264 (1994), 48.
- [20] KOKUBO T., KUSHITANI H., SAKKA S., KITSUGI T., YAMAMURO T., J. Biomed. Mater. Res., 24 (1990), 721.
- [21] YANG B.C., UCHIDA M., KIM H.M., ZHANG X.D., T KOKUBO., Biomater., 25 (2004), 1003.
- [22] SUL Y.T., JOHANSSON C.B., JEONG Y., ALBREKTSSON T., Med. Eng. Phys., 23 (2001), 329.
- [23] GONG D., GRIMES C.A., VARGHESE O.K., HU W., SINGH R.S., CHEN Z., DICKEY E.C., J. Mater. Res., 16 (2001), 3331.
- [24] MOR G.K., VARGHESE O.K., PAULOSE M., MUKHERJEE N., GRIMES C.A., J. Mater. Res., 18 (2003), 2588.
- [25] ROHRER G.S., *Structure and Bonding in Crystalline Materials*, Cambridge University Press, Cambridge, 2001, p. 365
- [26] KOKUBO T., Biomater., 2 (1991), 155.
- [27] HEALY K.E., DUCHEYNE P., J. Biomed. Mater. Res., 26 (1992), 319.
- [28] UCHIDA M., KIM H.M., KOKUBO T., FUJIBAYASHI S., NAKAMURA T., J. Biomed. Mater. Res., 64A (2003), 164.
- [29] TSUCHIYA H., MACAK J.M., MULLER L., KUNZE J., MULLER F., GREIL P., VIRTANEN S., SCHMUKI P., J. Biomed. Mater. Res., 77A (2006), 534.

Received 31 October 2006